Design procedures and guidelines for a novel self-centring concentrically braced steel frame based on displacement-based design approach

Design procedures and guidelines for a novel self-centring concentrically braced steel frame based on displacement-based design approach

H. Alwahsh[1], S. Salawdeh[2], Y. Jiang[1], J. Goggins[1,3]

[1] SFI MaREI Research Centre, Ryan Institute, School of Engineering, University of Galway, Galway, Ireland
[2] Department of Building & Civil Engineering, Atlantic Technological University, Galway, Ireland
[3] Construct Innovate, University of Galway, Galway, Ireland
email: H.alwahsh1@ universityofgalway.ie, Suhaib.Salawdeh@atu.ie, yadong.jiang@universityofgalway.ie
*Corresponding author email: ***jamie.goggins@universityofgalway.ie***

ABSTRACT: The introduction of the self-centring steel concentrically braced frame (SC-CBF) provides an innovative structural solution to seismic regions. Developed at the University of Galway, this innovative system possesses the unique ability to independently return to its original position after experiencing lateral deformation during an earthquake. Despite its significant benefits, it is noted that the lack of established guidelines in design codes, indicates that the development of the SC-CBF system is still in its preliminary phases.This article presents a Direct Displacement-Based Design (DDBD) methodology to design SC-CBFs. Flowcharts for conducting DDBD of the SC-CBF system are produced. The flowcharts offer a detailed set of steps to create user-friendly guidelines for constructing earthquake-resistant structures equipped with self-centring capabilities. This paper also encompasses a thorough analysis of a specific case study that revolves around a four-storey structure. This case study provides an in-depth evaluation of the design procedures, effectively demonstrating the tangible implementation of the methodology. The target displacement of the SC-CBF system at a 2.5% drift ratio resulted in a total base shear of 1382.6 KN after five analysis iterations. The SC-CBF system exhibits an effective period of 2.37 seconds and an equivalent viscous damping of 8.6 %. This comprehensive analysis will provide a deeper understanding of the design process for the SC-CBF system.

KEY WORDS: Self-centring, residual drift, direct displacement-based design, performance-based design, CBF, PT

1 INTRODUCTION

The field of structural engineering has witnessed several types of self-centring systems. These systems have captured significant attention and have undergone extensive study through both analytical and experimental studies. Self-centring technology's fundamental objective is to empower structures to return to their original positions following lateral displacements triggered by seismic or any lateral dynamic excitations.

These inventive systems achieve their aims by integrating various dissipative elements and devices. For instance, shape memory alloy dampers, energy-dissipating restraints, post-tensioned energy-dissipating connections, post-tensioned friction-damped connections and braces, energy dissipative braces, and yielding braces. Through the utilisation of the self-centring steel concentrically braced frame (SC-CBF) system, the comprehensive objective is to efficiently eliminate the residual deformations in structures exposed to seismic forces by employing replaceable braces. The continuous research and development in this realm hold the promise of increasing the seismic robustness and security of structures when confronted with earthquakes and other dynamic forces.

The novel SC-CBF system was initiated at the University of Galway by O'Reilly et al. [1]. This distinctive CBF system employed a horizontal self-centring approach. Theoretical and numerical portrayals of a single-story model were explored utilising the OpenSees software, aimed at understanding the behaviour of the Single-Degree-of-Freedom (SDOF) of the SC-CBF system. To assess the efficacy of the self-centring system, quasi-static pushover experiments were carried out at the Large Structures Laboratory of the University of Galway. The outcomes of these tests indicated a favourable correlation between the analytical predictions and the actual behaviour of the proposed SC-CBF system [2].

Goggins et al. (a), Goggins et al. (b), and McCready et al. [3-5] conducted a series of shake table tests. These tests were executed on a three-dimensional single-storey model at the Institute of Earthquake Engineering and Engineering Seismology (IZIIS) in R. North Macedonia, with the intention of building upon and extending the earlier research. The configuration of the SC-CBF and its connection behaviour, as based on O'Reilly and Goggins [6] is illustrated in Figure 1.

Notably O'Reilly et al. [1], provide valuable insights into the hysteretic behaviour of SC-CBF systems and offer clear guidelines for the design process of these systems. Figure 2 illustrates the flag-shaped hysteresis behaviour demonstrated by the combined system of the CBF and Post-Tensioned (PT) strands that constitute the SC-CBF system.

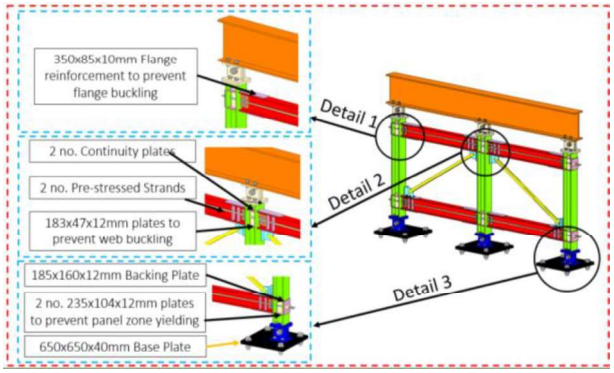

Figure 1. The details and experimental model of the rocking connection of the SC-CBF system.

2 DESIGN METHDOLODGY

The Direct Displacement-Based Design (DDBD) methodology serves as a design strategy aimed at determining the required strength of various structural systems. Its primary objective is to ensure the achievement of a specified performance state, characterized by predefined drift limits, when subjected to a designated level of seismic intensity. In the course of

employing this design approach, the fundamental base shear capacity demand necessary to withstand seismic forces acting upon the structures can be established. For a comprehensive explanation of the parameters in Figure 2, refer to O'Reilly et al. [1].

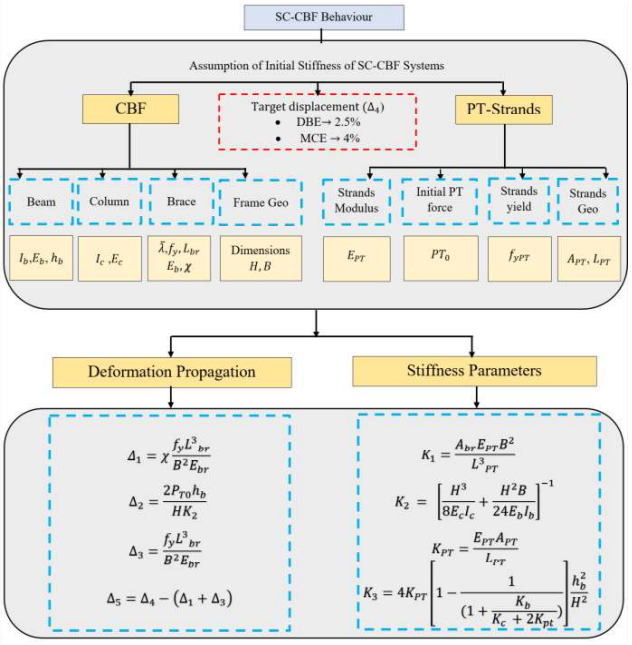

Figure 2. The flag-shaped hysteresis rules of the SC-CBF system [1] .

It is important to highlight that there is no specific expression available for Equivalent Viscous Damping (EVD) of the self-SC-CBF system, which allows the SC-CBF to naturally reposition itself after undergoing lateral displacements during seismic events. The remaining steps in the DDBD procedure align with the approach described by Wijesundara [7]. The base shear for the equivalent system is determined using the same methodology. The forces and displacements for the SC-CBF are obtained using the displacement-based equivalent lateral force procedure.

Based on the fundamental procedure of the DDBD design method, the transformation of MDOF to SDOF system is crucially important. To estimate the EVD for multi-systems, a combination or weighted-average rule can be used to combine the effects from the distinct systems. It is important to determine the equivalent damping for combined SDOF systems based on the proportion of performance for each system. Sullivan et al. and Maley et al. [8, 9] points out that work-based approaches generally result in conservative results for mixed systems. The EVD model for the SC-CBF system, which consists of both conventional CBF and PT strands, is a combination of both structural systems. This approach is in line with the proposals made by Sullivan et al. and Maley et al. [8, 9] and ensures consistency in the analysis of the SC-CBF system's behaviour. In the calculation of the EVD model for conventional CBF, the process considers both the system ductility (μ) and the normalized slenderness ($\bar{\lambda}$) of the brace member. [1]

Wijesundara [7] suggested using the limit of either 0.4 or 1.6 for $\bar{\lambda}$ in ductility equations. However, Salawdeh [10] demonstrated that a more accurate prediction for the EVD can be obtained without imposing these limits on $\bar{\lambda}$. Therefore, in the current study, no limits were imposed on $\bar{\lambda}$ .The main point highlighted by O'Reilly[2] that due to the combination of both CBF and PT systems in SC-CBF, the EVD model needs more investigation to consider the combined response of these two structural elements.

The common value of the elastic damping ratio is 0.05. Normally, the value of elastic damping for most materials range between 0.02 and 0.05. This study emphasises the crucial elastic behaviour of PT strands under seismic-induced strain elongation. Notably, the system exhibits no energy dissipation coefficient in its hysteretic response. Building upon the work of pioneers like Christopoulos et al. [11] , this research explores non-linear elastic behaviour in self-centring single-degree-of-freedom (SDOF) systems. Most of the researchers expressed the elastic damping ratio of 0.05 for the PT strands of the composite self-centring systems. In conclusion of that, the recommended value of the post-tension strands equivalent viscous damping ratio (ξ_{PT}) is 0.05 ([11, 12]). Therefore, The SC-CBF systems comprise the CBF system and the PT system that provides an extra energy dissipation response. The EVD expression for a SC-CBF ($\xi_{SC\text{-}CBF}$) consists of both the combined conventional CBF and the PT systems. The following equations express the EVD of the SC-CBF system:

$$\xi_{SC-CBF} = \kappa_{CBF}\xi_{CBF} + \kappa_{PT}\xi_{PT} \quad (1)$$

$$\xi_{SC-CBF} = \frac{\sum_{i=1}^{N} (V)\Delta_D \kappa_{CBF}\xi_{CBF} + \sum_{i=1}^{N} (V)\Delta_D \kappa_{PT}\xi_{PT}}{\sum_{i=1}^{N} V\Delta_D} \quad (2)$$

Where the damping coefficient for PT strands (ξ_{PT}) is set at 5%, based on O'Reilly et al. [1], it becomes evident that further investigation is necessary to address the uncertainties associated with the equivalent viscous damping coefficients. These coefficients encompass a range of critical parameters, including $V_{b,Ed}$ (representing the storey base shear), κ_{CBF} (indicating the frame shear resistance ratio), κ_{PT} (denoting the PT shear resistance ratio), ξ_{CBF} (characterizing the Equivalent Viscous Damping of the braces), and ξ_{PT} (representing the Equivalent Viscous Damping of the post-tensioning system).

In addition to that, Priestley et al., Salawdeh and Goggins , and Sullivan and Feinn [12-14] proposed a simple way to represent the effects of the higher modes on structure. Based on the equivalent lateral force, the distribution of the forces takes a linear pattern along the height of the structure. In addition to that, 10% of the total base shear will be located on the top of the roof level to consider the higher mode effects. While the remaining 90% of the base shear force is distributed to the all-floor level including the top floor.

The subsequent steps outline the DDBD methodology, which follows an iterative design approach. The accompanying flowchart offers a comprehensive breakdown of the sequential steps, offering engineers a straightforward and accessible framework for designing earthquake-resistant SC-CBF structures through this approach. The design process of DDBD, as developed within this study, applies to SC-CBF steel structures controlled by linear combined systems of EVD. The design procedure of the DDBD method presents a clear step to

assess the base shear of the self-centring system using a DDBD approach.

The procedure for DDBD is portrayed in Figure 3, where a target displacement and the effective stiffness of the structure have to be determined in order to calculate the base shear demand. Following the methodology outlined in Wijesundara [7] and O'Reilly et al. [1, 7], the equivalent single-degree-of-freedom (SDOF) system parameters (Δ_y , Δ_D H_e,and m_e) were determined. The structure is designed for a target displacement Δ_D ($\Delta_D = \Delta_y \times \mu$); where, $\Delta_{y,i}$ is the equivalent yield displacement at each storey which is calculated based on a tensile brace yielding and a rigid rotation of the connection resulting in shortening and elongation of the outer columns of the frame and μ is the equivalent displacement ductility as illustrated in O'Reilly et al. [1]. The target displacement value corresponding to the 'damage control' limit state is used in the design. The estimation of the equivalent viscous damping of the system, ξ, is established based on the ductility. Then, the effective period (T_e) of the structure is computed using the displacement response spectra generated for the estimated damping level and target displacement. Subsequently, the obtained T_e and m_e values contribute to the calculation of the effective stiffness (K_e) of the structure, as outlined in the equation as shown in Figure 3. The total base shear, represented by V_b, is calculated as the product of the effective stiffness and the target displacement ($V_b = K_e \times \Delta_D$). In order to account for the significant p-delta effect, an increase in the estimated base shear is applied. The distribution of the base shear among individual storeys is inversely related to their respective heights.

Figure 2 provides key parameters of the behaviour factors associated with the SC-CBF system, as proposed by the research conducted by O'Reilly et al. [15]. O'Reilly and Goggins [6] developed a design methodology for SC-CBF steel frames, which they validated through experimental pushover tests. Their study investigated a horizontal self-centring method and juxtaposed it with the vertical self-centring approach introduced by Sause et al. [16]. In the horizontal arrangement, a post-tensioned strand was deployed along the beams, as previously discussed. O'Reilly and Goggins [6] examined two initial values: 24% of the ultimate strength of the strands' capacity and 7% of the beam's axial yield strength. These values underwent comparison via experimental and numerical models, demonstrating a strong and positive correlation.

Alwahsh et al. [17] provides a flowchart that outlines the sequential steps for the seismic design methodology of the Steel SC-CBF system. This procedure aims to guide the design of earthquake-resistant structures that employ self-centring principles. Following the determination of demand base shear using either the Force-Based Design (FBD) or DDBD methods, the initial sections of the conventional system integrated within the self-centring CBF are proposed. The DDBD approach is favoured for its ease of application and performance-based nature, while the FBD method relies on structural dynamics and often yields stiffer and less cost-effective sections. The forthcoming case study will provide concrete evidence of the rigorous outcomes achieved through the utilisation of the DDBD method. Alwahsh et al. [17], presents a comprehensive design procedure for the self-centring system, incorporating conventional braced frame components and a PT system.

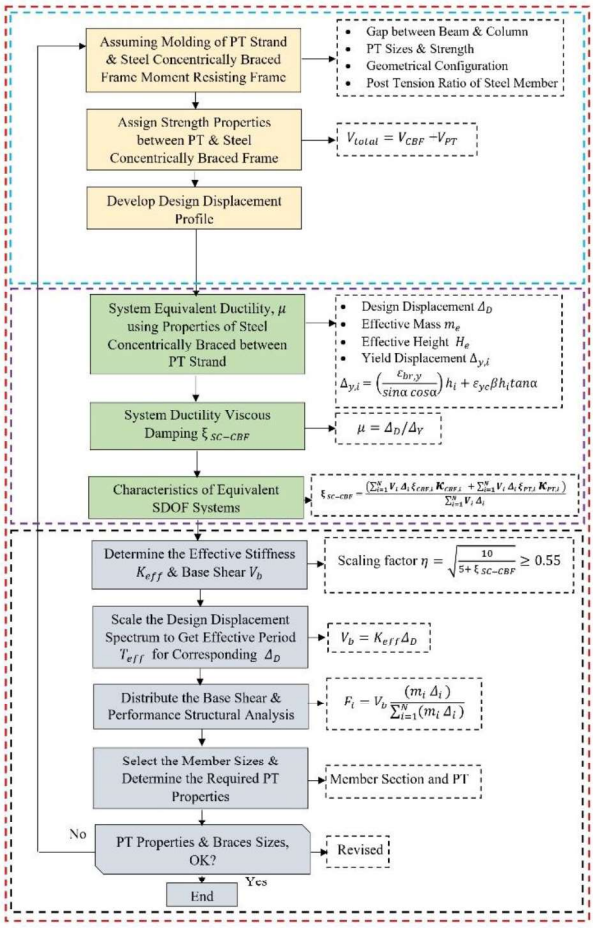

Figure 3. Preliminary design steps of DDBD method based on the design displacement approach method

3 CASE STUDY

3.1 Building Description

In this study, a 4-storey building is designed to investigate the DDBD for SC-CBFs. The building dimension is 24 × 24 m in plan. It consists of two lateral force-resisting SC-CBFs positioned along the exterior middle of the plan as shown in Figure 4. Each storey has a height of 3.2 meters. It is important to note that the interior frames are considered gravity frames, and their ability to resist lateral loads is not taken into account. To minimize torsional effects, symmetry has been implemented in the plan and elevation of the building. The connections between columns and beams are assumed to act as pin connections for the CBF structure. Additionally, all braces in the structural systems are attached to the flange of the beams to provide lateral resistance. The loads on the structure include the weight of the slab, finishes, partitions, claddings, and electrical and mechanical equipment, which collectively form a uniformly distributed load of 6.4 kN/m². The live load, following Eurocode 1, is considered to be 3 kN/m². S355 steel grade has been used for the main structural elements, such as beams and columns. S275 steel grade has been employed for gusset plates, while S235 steel grade has been utilised for the bracing members. It is important to note that all these steel

grades adhere to the standards set by EN 10219-1, BS EN 10025-2, and EC8 [18-20].

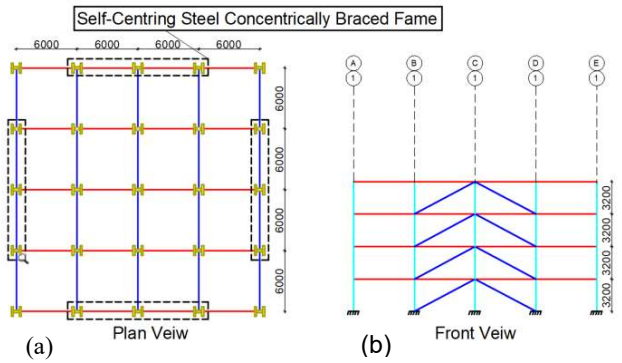

Figure 4. (a) Floor plan of the archetype building of CBF and MRF systems (b) The Elevation view of the CBF building (dimensions in millimetres)

3.2 Results and Discussions

Table 1 summarises the design storey displacements, Δ_{Di}, and yield storey displacements, Δ_{yi} .These were found to be 0.24 m, and 0.032 m, respectively. To design the building, first the substitute structure displacement, Δ_D, effective mass, m_e, effective height, H_e, and ductility, μ, are found. These were found to be 0.24 m, 715.1 tonne, 9.6 m and 7.54, respectively, as determined based on the design flowchart (Figure 3) of the SC-CBF system.

Table 1. The details of the design displacement profile and yield displacement profile.

Level	Height(m)	m_i(tonne)/fr*	δ_i	Δ_{Di}	Δ_{yi} (m)
4	12.8	214.5	1	0.32	0.042
3	9.6	214.5	0.75	0.24	0.031
2	6.4	214.5	0.5	0.16	0.021
1	3.2	214.5	0.25	0.08	0.010

*fr: floor

Then, the base shear is distributed to the floor levels, and the system's stability coefficient is evaluated following Sullivan et al. [21]. If $m_e g/H_e K_e > 0.05$, the stability the $P-\Delta$ effects are considered by amplifying the design storey displacements with the factor equal to $m_e g/H_e$. Calculations of the inter-storey drift of the P-Δ stability coefficients, θ, for each level of the building are done, as indicated in the provided flowchart. It is found that θ is less than 0.12 for all storeys as shown in Table 2 The maximum acceptable value of this coefficient θ is 0.3, so it is not necessary to consider the instability effects.

To obtain the damping level of the system, the EVD equations suggested by O'Reilly and Goggins [6] are used, which are a function of ductility, μ, and non-dimensional slenderness ratio, λ for CBF frame as well as the elastic damping of PT strands. The slenderness ratio is unknown at this stage of design an initial assumption of slenderness ratio is assumed to get the EVD. The elastic viscous damping of PT strands is 5%. The combined equivalent viscous damping (ξ_{SC-CBF}) for both systems at the initial stage of design, which is needed to evaluate the damping system at the beginning of the first iteration, is 0.22.

The effective period (T_e) corresponding to the design displacement is assigned using the displacement response curve. By referencing the displacement response spectra, the effective time period (T_e) of the structure for the target displacement in the first iteration is determined to be 3.02 seconds. Subsequently, the effective stiffness, K_e, is calculated using the provided formula, requiring knowledge of the structure's effective seismic weight, W_e. For the selected frame model, the value of W_e is 7015 kN, and the corresponding value of K_e is calculated to be 3095 kN/m.

The total base shear demand, denoted as $V_{b,Ed}$, is determined by multiplying the effective stiffness and the target displacement, resulting in an estimated value of 918 kN. This overall base shear is then distributed to each individual frame in inverse proportion to their height. Therefore, the base shear in each individual frame, represented as $V_{b,Ed}$ can be estimated using the formula provided in the flowchart. The calculated values for $V_{b,Ed,Frame}$ are 459.43 kN at each frame. The distributed forces and base shears at each floor level are presented in Table 2.

Table 2. Initial distribution of forces, shear, and the P-delta effect of the system

Level	H_i(m)	F_i (KN)	$V_{i,n}$ (KN)	P_i (Ton)	θ
4	12.8	422	422	2104.5	0.12
3	9.6	248	670	2104.5	0.07
2	6.4	165	836	2104.5	0.06
1	3.2	82	918	2104.5	0.05

Based on the initial assumption of the 50% participation ratio of the conventional CBF frame in the self-centring system. The rest of the shear force demand goes to the post-strands system. The re-distributed forces and demand base shear at each floor for the first iteration are constructed. Based on tension only diagonal bracings to resist the shear as suggested by CEN(2004) [22], the axial force in the brace, $N_{Ed,i,n}$, is found by dividing the floor shear, $V_{i,n}$, by the cosine of the angle of the inclined diagonal brace,α. The brace area, $A_{b,n}$, is found by dividing the axial force in the brace by the yield strength, f_y. All braces are chosen to be class 1 with a slenderness ratio $\lambda \leq 2$, as suggested by EC8 [22]. Table 3 shows the redistributed forces and the demand base shear for each floor at the initial iteration of the DDBD design steps.

Table 3. Initial calculation of force, shear, and the design of brace element (First Iteration).

Level	$V_{i,n}$(KN)	$N_{Ed,i,n}$(KN)	$A_{b,i,n}$(cm^2)	Section size
4	211	239	10.19	80x80x3.6
3	335	380	16.17	90x90x5.0
2	418	473	20.16	90x90x6.3
1	459	520	22.16	100x100x6.3

Thus, to check the adequacy of the selected braces sections. The design ductility should be less than the total ductility fractures μ_f obtained from Nip et al. [23].

Hot rolled carbon steel :

$$\mu_f = 3.69 + 6.97\bar{\lambda} - 0.05\frac{b}{t\epsilon} - 0.19\bar{\lambda}\frac{b}{t\epsilon} \quad (3)$$

Cold rolled carbon steel :

$$\mu_f = 6.45 + 2.28\bar{\lambda} - 0.11\frac{b}{t\epsilon} - 0.06\bar{\lambda}\frac{b}{t\epsilon} \quad (4)$$

Table 4 shows the ductility limits and ductility content for each brace section. The revised equivalent viscous damping is less than the trial one found by using the assumed slenderness ratio. Thus, the above procedure is carried out again using the new equivalent viscous damping to ensure adequate braces are determined. The combined equivalent viscous damping ratio for both systems at first iteration of analysis was evaluated.

Table 4.The design ductility of the braces (μ_f>7.54) compared with the total ductility fractures μ_f (First Iteration)

Level	Sections	λ_n	HR-CS*	CR-CS**
4	80x80x3.6	2.32	8.97	8.21
3	90x90x5.0	2.09	10.24	11.52
2	90x90x6.3	2.12	12.04	11.56
1	100x100x6.3	1.90	10.43	10.86

*(HR-CS) Hot Rolled - Carbon Steel
**(CR-CS) Cold Rolled - Carbon Steel

Consequently, the updated equivalent viscous damping is lower than the initial trial value obtained through the assumed slenderness ratio. Thus, the above procedure is carried out again using the new equivalent viscous damping to ensure adequate braces are determined. The trials are finished when the same brace sizes are found to be adequate in two sequential trials. Table 5 shows the combined equivalent viscous damping ratio for both systems at first iteration of analysis. This calculation is based on weighted average multi-system equivalent viscous damping analysis. The equivalent viscous damping in the first iteration ξ_{SC-CBF} is 0.084. The same procedure has been done for all iterations of the based shear calculations until the equivalent viscous damping is established.

Table 5.The combined system of the new EVD ratio of the system (ξ_{sc-CBF})

Level	Brace Sections	$\xi_{CBFi,n+1}$	$V_{i,n,CBF}$ (KN)	$V_{i,n,PT}$ (KN)
4	80x80x3.6	0.105	3.54	1.69
3	90x90x5.0	0.120	4.83	2.01
2	90x90x6.3	0.118	3.94	1.67
1	100x100x6.3	0.133	2.44	0.91

In the fifth iteration of the self-centring combined system, the equivalent viscous damping for the SC-CBF system is represented as ξ_{SC-CBF} = 0.086. The updated braces and design parameters for the SC-CBF frame, as determined in the final iteration of the design procedure as per Figure 3, yield the necessary steps and requirements for achieving DDBD compliance. These steps and requirements are essential for ensuring the seismic performance and self-centring behaviour of the SC-CBF system. It is important to highlight that in this context, the maximum brace overstrength factor, represented as Ω_i, was intentionally established at a value of 20%, as explicitly outlined in Table 6.

Table 6. Final trial results of designing sections for braces.

Level	$V_{i,n,CBF}$ (KN)	$N_{Ed,i,n}$ (KN)	$A_{b,n}$	λ_n
4	318.0	360.4	15.34	2.10
3	504.6	571.9	24.34	2.18
2	629.1	712.9	30.34	1.99
1	691.3	783.5	33.34	1.99

Upon completing the design process, it is possible to draw conclusions and present the results. In this example, the braces were selected after the fifth trial (i.e., n = 5), as shown in Table 6. All braces meet the requirements according to the CEN(2004) [22]. The sections are to be Class 1 with a slenderness ratio $\lambda \leq 2$. Brace members were chosen carefully to represent the design values as closely as possible, as the purpose of this design is to verify the design methodology, where the maximum brace overstrength factor, Ω_i, was 20%.Table 7 gives the summary of the effective height, effective period, effective stiffness, and total base shear force and the equivalent viscous damping for five iterations.

Table 7. The summary list of the effective period, effective stiffness, and total base shear force.

No. Iterations	T_e(sec)	K_e(KN/m)	V_b(KN)	ξ_{SC-CBF}
First	3.02	3097.87	918.87	0.084
Second	2.35	5116.31	1403.25	0.095
Third	2.51	4484.66	1251.7	0.089
Fourth	2.43	4784.81	1323.73	0.086
Fifth	2.37	5030.14	1382.61	0.086

The calculation of the overall brace sections in the SC-CBF system was conducted employing the DDBD method, as outlined in Figure 4. It was assumed that 50% of the base shear is counteracted by the PT strands system (designated as K_{pt} = 0.5), while the remaining portion is resisted by the CBF frame. As a result, the self-centring concentrically braced frame system operates cohesively to withstand the entirety of the base shear, considering the joint rocking assumption. Table 4 provides more specific information about the braces utilised at each storey level.

Initial assumptions for system parameters were made, as depicted in Figure 2. The PT elements were designed with a yield stress ($f_{y,PT}$) of 1770 MPa and a modulus (E_{PT}) of 195 MPa. The initial PT force applied to the strands (PT_0) was assumed to be $0.25f_{y,PT}A_{PT}$ where A_{PT} represents the cross-sectional area of the PT strands. Assuming pinned connections at the CBF, the beams and columns were found to have adequate capacity according to EC8. The initial cross-sectional area of the PT strand (A_{PT}) was assumed to be $0.05A_{b,n}$. The selected PT strands consist of 7-wire standard strands with a nominal diameter of 15.2 mm and a nominal area of 139 mm². The PT forces that developed due to the target lateral displacement at each floor level. These forces were compared against the shear resistance capacity of the PT strands ($V_{i,Rd,PT}$). It is critically important to ensure that the design force in the PT strand (PT_{Ed}) does not exceed 75% of the design capacity of the PT strand (PT_{Rd}). The analysis of the maximum capacity of the PT strands was preceded by assessing the total design shear ($V_{i,Ed,5}$) exceeding zero to confirm the characteristic behaviour resembling a flag shape. Table 8 lists the conclusive outcomes of the SC-CBF components, encompassing primary elements such as beams and columns, braces, and the number of strands.

Table 8. Sections and drift limits of four-storey building for SC-CBF system using DDBD method.

Level	Braces	Beams	Columns	Strand No.
4	90x90x5.0	IPE600R	HE400M	8
3	90x90x8.0	IPE750x161	HE400M	10
2	100x100x10	IPE750x222	HE400M	10
1	100x100x10	IPE750x222	HE400M	12

4 CONCLUSION

This paper provides a methodology detail for a comprehensive and user-friendly approach to design SC-CBFs earthquake-resistant structures. It is employed after determining the demand base shear using the DDBD methodology. The steps include selecting design parameters, identifying self-centring system components, creating a structural model with appropriate analysis, assessing displacement demands, and ensuring ductility and capacity. The lateral forces acting on the structure are entirely resisted by braces and rocking connections. These components are specifically designed to facilitate self-centring behaviour, meaning that after experiencing lateral displacements during an earthquake, the structure is capable of returning to its original position due to the flexibility and energy-dissipating properties of the braces and rocking connections. Despite this self-centring behaviour, the main structural elements, including columns, beams, and PT strands, maintain their elastic behaviour, ensuring that they remain within their elastic limits and can efficiently support the loads without undergoing permanent deformation.

The design process included defining performance goals for the structure under the DBE seismic hazard level. These goals encompassed interstorey drifts, residual drifts, and the behaviour of beams, columns, and post-tensioned elements. An example of a 4-storey SC-CBF was designed using the DDBD approach to meet these performance goals, considering the interactions between different structural components. The study demonstrated that the performance goals were successfully achieved for various seismic hazard levels, showing the effective integration of DDBD into a performance-based design framework. The promising outcomes indicate the SC-CBF's performance at different intensity levels and the efficacy of the DDBD procedure within a performance-based design framework.

ACKNOWLEDGMENTS

This research was funded by the Seismology and Earthquake Engineering Research Infrastructure Alliance for Europe (SERA-H2020-INFRAIA-2016-2017/H2020 INFRAIA-2016-1) under grant agreement No. 730900 for the project "Investigation of Seismic Deformation Demand, Capacity and Control in a Novel Self-Centring Steel Braced Frame (SC-CBF)." The first author acknowledges the support of Science Foundation Ireland through the Career Development Award programme (Grant No. 13/CDA/2200) and the MaREI Centre (Grant No. 12/RC/2302_2). This research was also supported by the Marine Institute, funded under the Marine Research Programme by the Government of Ireland (PDOC/21/03/01).

REFERENCES

[1] O'Reilly G, Goggins J, Mahin S. (2012) Development of a Novel Self-Centering Concentrically Braced Frame System for Deployment in Seismically Active Regions.

[2] O'Reilly GJ. (2013). 'Development of a Novel Self-Centering Concentrically Braced Frame System'. MSc Thesis, National University of Ireland, Galway,Ireland.

[3] Goggins J, Jiang Y, Broderick BM, Salawdeh S, O'Reilly GJ, Elghazouli AY, Alwahsh H, Bogdanovic A, Rakicevic Z, Gjorgjjev I, Poposka A, Petreski B, Markovsk I. (2020). Experimental testing of a novel self-centring steel braced frame on the shake table in Dynlab-IZIIS`.*Proceedings of the 17th World Conference on Earthquake Engineering (17WCEE)*. Septemper 13-18 2020, Sedni, Japan.

[4] Goggins J, Jiang Y, Broderick BM, Salawdeh S, O'Reilly GJ, Elghazouli AY, Alwahsh H, Bogdanovic A, Rakicevic Z, Gjorgjjev I, Poposka A, Petreski B, Markovsk I. (2020). Shake Table Testing of Self-Centring Concentrically Braced Frames`.*Proceedings of EUROSTEEL*. Septemper 2020, Sheffield, UK.

[5] McCready P, Jiang Y, Salawdeh S, AlWahsh H, Broderick B, Goggins J. (2020) Performance validation of a self-centring steel structure using robust data sets from shake table testing.

[6] O'Reilly G, Goggins J. Comparing the seismic performance of concentrically braced frames with and without self-centering behaviour. *In Structures and Architecture*. CRC Press, 2013: 1585-92.

[7] Wijesundara K. (2009) Design of concentrically braced steel frames with RHS shape braces. *Università degli Studi di Pavia & Istituto Universitario di Studi Superiori*.

[8] Sullivan TJ. (2013) Direct displacement-based seismic design of steel eccentrically braced frame structures. *Bulletin of Earthquake Engineering*. 11: 2197-231.

[9] Maley T, Sullivan T, Pampanin S. (2011) Seismic design of mixed MRF systems. *ROSE School PhD thesis, IUSS Pavia, Pavia, Italy*. 96-105.

[10] Salawdeh S. (2012) Seismic design of concentrically braced steel frames.

[11] Christopoulos C, Filiatrault A, Folz B. (2002) Seismic response of self-centring hysteretic SDOF systems. *Earthquake engineering & structural dynamics*. 31(5): 1131-50.

[12] Priestley M, Calvi G, Kowalsky M. (2007) Direct displacement-based seismic design of structures. *NZSEE conference*. 1-23.

[13] Salawdeh S, Goggins J. (2016) Direct displacement based seismic design for single storey steel concentrically braced frames. *Earthquakes and Structures*. 10(5): 1125-41.

[14] Sullivan GM, Feinn R. (2012) Using effect size—or why the P value is not enough. *Journal of graduate medical education*. 4(3): 279-82.

[15] O'Reilly G, Goggins J, Mahin S. Development of a Novel Self-Centering Concentrically Braced Frame System for Deployment in Seismically Active Regions. *In Bridge and Concrete Research in Ireland*. 2012.

[16] Sause R, Ricles JM, Lin Y-C, Seo C-Y, Roke D, Chancellor B. (2010) Self-centering damage-free seismic-resistant steel frame systems. *Joint Conference Proceedings–Seventh International Conference on Urban Earthquake Engineering and Fifth International Conference on Earthquake Engineering*.

[17] Alwahsh H, Salawdeh S, Yadong J, Goggins J. (2024). Force-based design of a novel self-centring concentrically braced steel structure – a case study. 18th World Conference on Earthquake Engineering *18th World Conference on Earthquake Engineering (18WCEE)*. 30th June-5th July., Milan,Italy.

[18] EN 10219-1. Cold formed welded structural hollow sections of non-alloy and fine grain steels. In: *Part 1: Technical delivery conditions Irish Standard*. 2006.

[19] BS EN 10025-2. Hot rolled products of structural steels. Technical delivery conditions for non-alloy structural steels. In: *BSI*. 2004:38.

[20] CEN. Cold formed welded structural hollow sections of non-alloy and fine grain steels. 1. Technical delivery requirement. 2. Tolerances, dimensions & section properties.: EN10219-1:1997 1997.

[21] Sullivan T, Priestley M, Calvi GM. *A Model Code for the Displacement-Based Seismic Design of Structures DBD12*, 2012.

[22] CEN. Eurocode 8, design of structures for earthquake resistance – Part 1: General rules, seismic actions and rules for buildings. EN 1998-1:2004/AC:2009 2004.

[23] Nip K, Gardner L, Elghazouli A. (2010) Cyclic testing and numerical modelling of carbon steel and stainless steel tubular bracing members. *Engineering structures*. 32(2): 424-41.